Comparing the Period-Luminosity relationships in variable stars

Daniela Romero
Uppsala Universitet
daniela.romero1230@gmail.com

June 2017

Abstract

There are four Period Luminosity relations from three sources, [3, 5, 9, 11], that are compared for their accuracy in calculating distances and to see how much uncertainty has to be considered when calculating other distances based on these. Here, the relations are compared by using each to calculate and compare the distances of the stars: BK Vir, L2 Pup, R Hor, R Hya, R Lep, and RR Aql; along with using data from AAVSO and SIMBAD in the calculations. The relations have an uncertainty that ranges from about 30%-40%, except for the relation from [9] that has an uncertainty of 90%

1. Background

Pulsating stars vary in observed brightness, they are a type of intrinsic variable star. They are used as standard candles (objects with a defined absolute magnitude that does not vary with age or distance) to determine the distances of objects around them, including objects within and beyond the galaxy. This is done by determining their own distance using the linear relationship between the period of their pulsations and the intrinsic luminosity: the Period-Luminosity relationship. Variable stars are also observed to research stellar properties and evolution [2].

The brightness pulsations themselves are caused by the physical property of the star - the surface layers periodically expand and contract. It is the rate that the radiation is exiting the star that changes the brightness, the actual fusion rate does not influence the pulsation. The outer layers expand when the outward pressure of the radiation becomes greater than the gravitational force, then when they have expanded to a certain point, the pressure is reduced but the layers of the star continue to expand, although at a slowing rate. The gravitational force becomes greater and the layers contract in, consequently increasing the pressure, causing the cycle to continue. This is in turn based on the the mass and evolutionary stage of the star, thus there are different types of Variable stars.

The types can be classified based on their light curves, which are based on amplitude and regularity, or their spectral type. The types of pulsating variables include Cepheid, RR Lyrae, RV Tauri, Miras, and Semi-regular and Irregular variable stars [1]. Cepheid are population I supergiants in the spectra class F-K with a short period of 1-50 days and an amplitude of .1 - 2.5 magnitudes. RR Lyrae stars have a shorter period (less than a day) and vary in brightness less. They are commonly found in globular clusters, so are used to determine the distances to these. Mira variables are large giants with long periods that lose mass to stellar wind, the brightness for these stars can vary by about 6 magnitudes (visual) and they mostly emit in the infrared. Other long period varible stars include Semi-regular and irregular stars.[6]

Miras, Semi-regular and irregular variables are Asymptotic Red Giants, AGB, rare stars with long period variations, they typically have a period of 100-1000 days. The AGB branch is where stars are at the end of their lives, when Helium and Hydrogen are burning in a shell around the core. These are rare stars that have evolved into red giants from stars with a mass ranging from .8-8$M_{\odot}$. These stars are only in the AGB stage for a small part of their lives compared to earlier stages. During this time, the stars have a Carbon-Oxygen core, and shells of helium and hydrogen where fusion takes place. The AGB stars have another long term thermal pulsation, where it is powered primarily by burning the helium shell. The pulsation stars when most of the fusion shifts over to the hydrogen shell and more helium is produced. The helium builds up, ignites, and forms a helium flash and produces C^{12} that mixes with the O^{16} in the convective envelope [8, 7]. This is part of the evolution of the star, and is on a much longer scale.

AGB stars can be classified based on the ratio of carbon to oxygen in their spectra, or based on the regularity of their light curves. The classes based on spectra are M, S, and C types; M stars have an atmosphere with mostly oxygen molecules with a C-O ratio less than 1 and the carbon is mostly found

in CO molecules, AGB stars are classified as S stars when more carbon is dredged up and the C- O ratio increases to about 1, and when the ratio has increased above 1 so that the atmosphere has mostly carbon molecules [7]. It is easier for carbon stars to for in low metallicity environments because less carbon needs to be dredged up to the atmosphere. [8]

Mira variables have the most regular period compared to Semi-regular and irregular variables, with a period of 100 - 500 days and a very large amplitude. Their regularity means they can be used as standard candles for distances in the galaxy and to nearby galaxies. Miras are at the edge of the AGB stage, just before releasing its layers to a planetary nebula. They are also losing mass from the convective surface, causing a shell of grains and dust to form around the star, this rate can be modeled from the distance to the star. Because of this, they can also be used to gather information about stellar evolution of low to intermediate mass stars, composition of interstellar medium, and the structure of the Milky Way [10]. Although the way matter is lost from the surface is not fully understood. Some observations of the mass loss rate can show that it is related to the pulsation of the star; so the PL relation can give insight on this. Also, information about the outer atmosphere can provide clues to how the grain forming process happens; the dust formation itself may also not be uniform [4].

The atmosphere of Miras can also vary in size depending on the wavelength at which they are observed, although they are, in both cases, very extended. The large atmosphere makes it difficult to determine just where to start measuring the diameter of star, models even show the star to not be circular when it is observed in the optical wavelength. This may be caused by large star-spots that, because of the nature of the instruments used, cannot be properly resolved. The atmosphere also has large convection cells and clouds of material that rise and fall back to the surface that support the explanation. Other possibilities are that the atmosphere is flattened by the rotation of the star, or if it has non-radial pulsation [4].

There are different classes of Miras, where they are classified based on their atmospheres similarly to the classification used for AGB stars in general. They can be O or C type; O type Miras have majority of oxygen molecules, within this type, there are two other classes: M and S. M types have the TiO molecule dominant in the absorption band, and S types have ZrO as well as some TiO. In another case, an O Mira with a longer period would be subclassified as an OH/IR type; these are identified by the OH molecule in their spectra. OH/IR stars are mostly visible in the infrared because of their low temperature and significant circumstellar extinction. There are also OH masers within the O Mira and OH/IR Mira classes. And C type Miras have mostly carbon molecules. The variation is cause by different amounts of Carbon being dredged up from fusion in the helium shell. The different types of Miras also produce different compositions of dust grains; the grains in C Miras are mostly carbon compounds, compared to O Miras, which have mostly silicates [4].

2. The problem

There is an uncertainty in the calculation for the distances to stars from the period-luminosity relationship derived from observations of Miras. This is due to there being different variations of the P-L relations used, and they each are derived using different methods. The relations vary based on how the observations were made, and which kinds of Mira stars were observed.

The difference in the relations come from the discrepancy in using a different method of determining distances for the stars observed. In some methods, the relation was derived for Miras in the LMC, where the distance is known, and the same distance value of the LMC was used to determine the relation. The relation is then applied to Miras in the Galaxy.

Another way to get a value for the distance of the stars to determine a relation is by using parallax data from *Hipparcos*. The issue with this method is that the parallax cannot be accurately determined for stars with a period over 400 days for O Miras and for C Miras if the relation is derived from a broad range of periods.[3] This is because the period of Mira stars is a function of their initial mass, so the mass lost to the surface of the star and the variation in size make it appear to be moving around. Also, parallaxes are measured in the optical spectrum, which is obscured from circumstellar extinction.

Although there is a way around this issue for O Miras if the intrinsic color is estimated from the period-color relation. The extinction can be corrected and then the K band relation can be applied [10]

Since each variation of the observations used derives a slightly different P-L relation, there will be a variation in the distances calculated; the amount of variation in the distances calculated is the problem that is addressed here. This also creates an issue with estimating the mass loss rates and the abundances of the stars [8].

3. The Period - Luminosity Relation

The relation is given by:
$M = \rho \log(P) + \delta$
The ρ and δ values vary depending on which method is used to derive them. The absolute magnitude, M, of the star is calculated from observing the period, P, from the specific star. Along with the zero point, δ, and the slope of the equation ρ.

There are different relations if observations are made from Miras in the Galaxy or the LMC, although ρ has been seen to apply to both [10]. The zero point is adjusted from the LMC to the Galaxy

Observations of the star are more accurate if they are done in the K band spectrum instead of the visual spectra or for the bolometric magnitude. This is because of the K band is least affected by extinction, specifically by the circumstellar dust shell [10]. The zero point can vary based on which stars the observations are made from, whether they are from the LMC or the Galaxy, since the zero point can be dependent on metallicity.

Further, the relation can be different if determined from OH/IR stars (if they can be properly observed despite their high mass-loss rate) compared to Mira stars. So the relations derived are based on just Mira variables.

4. Specific Period-Luminosity relations

There are a few versions of the P-L relation, each with different observation methods. These are the relations commonly used in calculating distances and how they are derived:

4.1.

In the relations derived from Feast et al. (1989) [3] the Miras observed were 29 O type and 20 C type from the LMC, they are from time-averaged J, H, K, and m_{bol} magnitudes. The bolometric magnitude values were calculated from dereddened values of the JHK magnitues by interpolating from a blackbody curve. Observations of the stars were used to produce light curves with periods ranging from 117 to 420 days; there are six additional stars with periods over 420 days that have been separated.

The relations are derived with least-square fits. For O Miras there is a good relation in the K band, but there is more scatter for J and H. The C Miras also had a good K relation, but with some more scatter; omitting shorter period Miras yields a better relation. Both classes still had a similar relation for the K band. The combined relation is:

$$M_K = -3.57 \pm 0.16 \log(P) + 1.15 \pm 0.39 \qquad (4.1)$$

Feast et al. (1989) also determines period-color and period-color-luminosity relations. It was also noted that O Miras are present in metal rich globular clusters, their distances can be used to calibrate the zero point. Although knowing the distances to the globular clusters are dependent on the absolute magnitudes of RR Lyrae variables.

4.2.

Groenewegen and Whitelock (1996) [5] derived a PL and PK (bolometric and K band) relation from 54 C Miras with a period between 150-520 days in the LMC using a two-step process. The relations are applied to the Galaxy by assuming the same slopes can be used and the zero points from shifting the relations. For the zero points, it has to be assumed that the distance modulus is 18.5 and there is no correction for metallicity differences. The PL relation is derives similarly to in Feast et al. (1989). The relations were derived from information that was also used in Feast et al. (1989), Hughes (1989), Hughes & Wood (1995), and Reid et al. (1995).

There are two stars with a period of 657 and 486 days that clearly deviate from the data, so they are excluded. The PL relation is steeper than in Feast et al., but is more similar for the PL K relation.
The relation is:

$$M_K = -3.56 \pm 0.17 \log(P) + 1.14 \pm 0.42 \qquad (4.2)$$

4.3.

The previous methods used stars for the LMC for the relation because their distance is known. In the relation derived in Knapp et al. (2003), K band luminosities from Galactic long period variables (LPV) were used instead of LMC Miras. It is determined this way both because it is questioned if the same slope can be used, as well that the zero-point is actually dependent on the metallicity difference between the LMC and the Galaxy.

The values for K magnitudes are from other literature along with COBE measurements. The distances used were reprocessed parallax values from *Hipparcos*. The stars used included Miras, SRa, and SRb, along with M, S, and C spectral classes. It was found that there was no difference in the relation based on spectral class, but there is a difference for the type of LPV used. The relation derived from the Miras here is consistent with the relation from Feast et al. (1989).

It is interesting to note that there was a good relation derived from SRb stars, although the slope is very different; compared to SRa stars, which seem to vary between Miras and SRb. So the pulsation for these stars changes from being like Miras to SRs. The relation derived from least-square fits is: [9]

$$M_K = -3.39 \pm 0.47 \log(P) + 0.95 \pm 3.01 \qquad (4.3)$$

4.4.

The final PL relation discussed is derived in Whitelock et al. 2008 [11]; it is based from re-analyzing data from AGB stars in the LMC to get a K band relation. The slope of the relation is applied to Galactic Miras, and the zero point is found using *Hipparcos* parallaxes along with VLBI parallaxes. The VLBI parallaxes are used for OH masers, but are very useful for stars with high mass loss rates that would otherwise not have good parallax values. The relation is from O Miras; a relation for C Miras is also found, but it has more uncertainties. The slope between both classes is not significantly different and the zero point varies by 0.093 ± 0.032. Here it is also found that the metallicity difference is not enough to have a significant affect on the zero point.

They use 31 O Miras from the LMC with a period less than 420 days for relation a; and for relation b, for the galaxy, is determined by using the same slope, and solving for the zero point:

$$M_K = -3.51 \pm 0.20 \log(P) + 1.20 \pm 0.06 \quad (4.4a)$$

$$M_K = -3.51 \pm 0.20 log(P) + 1.10 \pm 0.07 \quad (4.4b)$$

5. Determining Distances

With the absolute magnitude calculated, the distance can be calculated. Depending on which relation is used, this would yield a variation in the distance values. To see just how much this difference is, a set of Miras are chosen to compare.

5.1. Measuring the periods

The stars used are: BK Vir, L2 Pup, R Hor, R Hya, R Lep, and RR Aql. To begin, their light curves are plotted from observation in Visual and V band acquired from the AAVSO database. Other stars with limited observations that did not produce a clear plot were excluded. From the plots, the period was determined by counting the distance between a few peak brightnesses, and taking an average of the days.

There are limited observations for some of the plots; even for those that have enough information to measure a period, there is some uncertainty in the value. For some plots there is a wide spread as to where the peaks are that are used to measure the period. There are two stars not mentioned, BK Vir and U Hya, that have plenty of data, but the light curve itself is not clear enough to see where the peaks are, these light cures are shown in the appendix.

The plot of BK Vir is an example of where there is significant uncertainty; some peaks it is rather clear where their maximum is, but for other peaks there are a few stars that do not appear to be the maximum point. It is estimated that the actual peak would be somewhere between the highest points (in terms of the date measured).

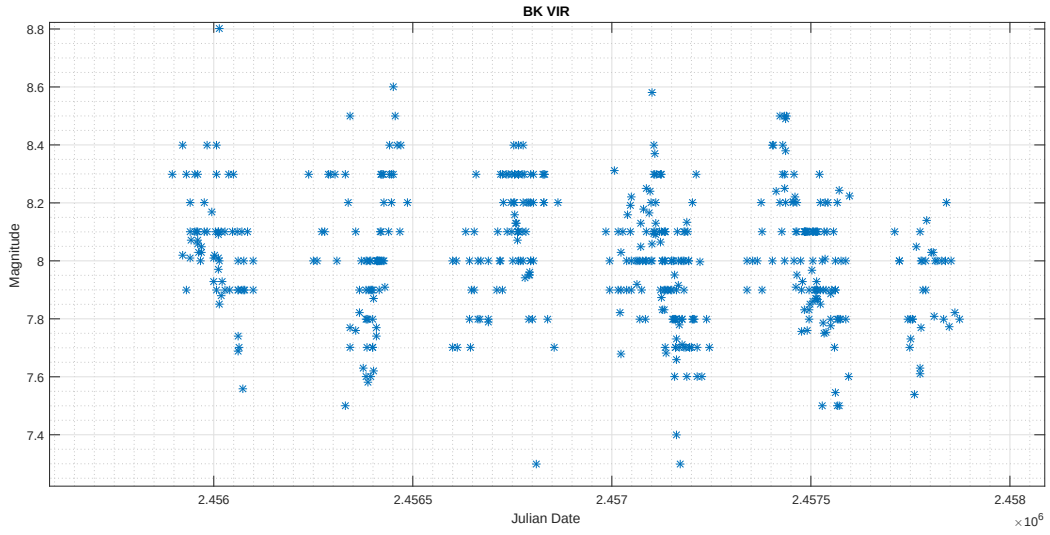

Figure 1: *BK Vir light curve*

It is clear that in Figure 1 there are 6 peaks, but each of them are uncertain by some different amount of dates. The following table shows the uncertainty in days for each peak.

Peak	Julian Date
1	2457874± 30
2	2457430 ± 9
3	2457109± 4
4	2456764 ± 12
5	2456397 ± 54
6	2456002± 16

Table 1: *Bk Vir peak uncertainty*

For the first peak, the uncertainty is rather high; it is measure as being somewhere between the two top outer points. There are 66 days between these two points, it assumed the peak could be in the middle. It is quite a large assumption, so the uncertainty for the date of the peak would be, at most, about 30 days. The 2nd, 3rd, 4th and 6th peaks look more certain, with what appears to be just a small area where the actual peak would be. The 5th peak has an uncertainty similar to the first. Other plots have better measurement and are much clearer, like the R Hya light curve in Figure 2:

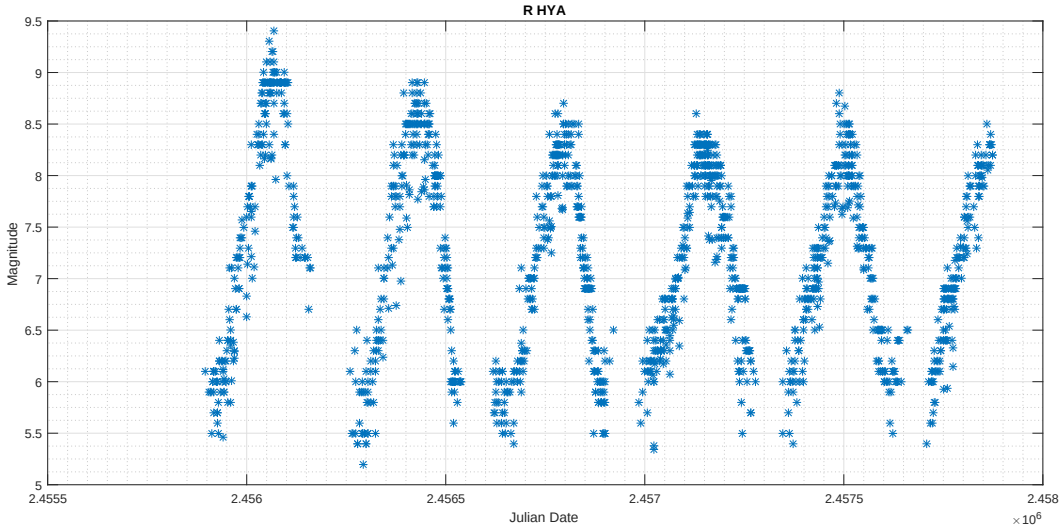

Figure 2: *R Hya light curve*

For R Hya, the 5th peak has the most uncertainty, for the others, it is minimal.

Peak	Julian Date
1	2457860± 9
2	2457487± 5
3	2457129± 10
4	2456795 ± 5
5	2456432± 16
6	2456068± 6

Table 2: *R Hya peak uncertainty*

The rest of the plots and the uncertainties are shown in the appendix.
The period for each star is individually calculated with consideration to the uncertainty of the dates to calculate a maximum and minimum period for each peak. Each period for each peak is averaged along with its uncertainty to calculate the period for the star.

Star	Period
BK VIR	374 ± 40
L2 PUP	144± 16
R HOR	391 ± 13
R HYA	358± 14
R LEP	437± 18
RR AQL	393± 105
SW VIR	315± 31

Table 3: *The approximate period for the stars in days*

5.2. Calculating the absolute K magnitude

The period is then used in each PL relation to calculate the absolute magnitude of each star with consideration to the uncertainties.

The absolute K magnitudes are calculated:

PL Relation	M_k
4.1	-8.03±.97
4.2	-8.02±1.02
4.3	-7.79±4.38
4.4a	-7.83±.74
4.4b	-7.93±.75

Table 4: *Absolute K magnitudes for BK Vir*

PL Relation	M_k
4.1	-6.55±.91
4.2	-6.54±.96
4.3	-6.38±4.19
4.4a	-6.38±.66
4.4b	-6.48±.67

Table 5: *Absolute K magnitudes for L2 Pup*

PL Relation	M_k
4.1	-8.11±.86
4.2	-8.09±.91
4.3	-7.84±4.28
4.4a	-7.90±.63
4.4b	-8.00±.64

Table 6: *Absolute K magnitudes for R Hor*

PL Relation	M_k
4.1	-7.97±.86
4.2	-7.95±.91
4.3	-7.71±4.27
4.4a	-7.77±.63
4.4b	-7.87±.64

Table 7: *Absolute K magnitudes for R Hya*

PL Relation	M_k
4.1	-8.28±.88
4.2	-8.38±.93
4.3	-8.00±4.31
4.4a	-8.07±.65
4.4b	-8.17±.66

Table 8: *Absolute K magnitudes for R Lep*

PL Relation	M_k
4.1	-8.07±1.23
4.2	-8.06±1.28
4.3	-8.00±4.31
4.4a	-7.87±.99
4.4b	-7.97±1.00

Table 9: *Absolute K magnitudes for RR Aql*

PL Relation	M_k
4.1	-7.77±.94
4.2	-7.75±1.0
4.3	-7.53±4.33
4.4a	-7.57±.71
4.4b	-7.67±.72

Table 10: *Absolute K magnitudes for SW Vir*

5.3. Calculating the distance

With the absolute k magnitude and the apparent K magnitude, the distance modulus, μ, is calculated and used in the distance equation:
$d = 10^{1+\left(\frac{m-M-A}{5}\right)}$, $\mu = m - M$
And the distance equation is written as:
$\mu = 5(log(d) - 1)$

Then set for the distance:
$d = 10^{\frac{\mu}{5}+1}$
The distance of the star is calculated, and the different relations are compared based on the distances. The values for the apparent magnitudes are take from the SIMBAD astronomical database:

Star	m_k
BK VIR	-.91
L2 PUP	-1.97
R HOR	-1.00
R HYA	-2.51
R LEP	+.10
RR AQL	+.31
SW VIR	-1.79

Table 11: *Apparent K magnitudes*

PL Relation	Distance (pc)
4.1	292.39±122.57
4.2	292.58±128.14
4.3	909.056±877.43
4.4a	256.30±84.11
4.4b	268.78±89.31

Table 12: *BK Vir distance*

PL Relation	Distance (pc)
4.1	89.76±35.56
4.2	90.18±37.46
4.3	267.87±256.87
4.4a	79.76±23.52
4.4b	83.63±25.01

Table 13: *L2 Pup distance*

PL Relation	Distance (pc)
4.1	285.24±107.41
4.2	285.15±112.96
4.3	853.73±821.22
4.4a	250.05±70.58
4.4b	262.18±75.11

Table 14: *R Hor Distance*

PL Relation	Distance (pc)
4.1	133.42±50.24
4.2	133.34±52.84
4.3	399.39±384.04
4.4a	117.50±33.16
4.4b	123.20±35.29

Table 15: *R Hor Distance*

PL Relation	Distance (pc)
4.1	513.72±197.49
4.2	542.84±219.24
4.3	1545.59±1488.31
4.4a	449.96±130.81
4.4b	471.80±139.14

Table 16: *R Lep Distance*

PL Relation	Distance (pc)
4.1	552.15±283.22
4.2	556.82±294.66
4.3	1702.52±1639.43
4.4a	478.25±204.10
4.4b	501.78±216.02

Table 17: *RR Aql Distance*

PL Relation	Distance (pc)
4.1	173.30±73.30
4.2	172.39±74.21
4.3	525.95±506.81
4.4a	150.94±47.67
4.4b	158.29±50.64

Table 18: *SW Vir Distance*

6. Summary

It is clear that there is huge uncertainty in the distances from all of the relations, although some are much more than others. Some uncertainty is due to measuring the period, however across the different stars, the percent of uncertainty for each relation is somewhat similar. Across each star, for the relations, the average uncertainties are as follows:
For the first relation: 41.87%.
Second relation: 43.55%
And the fourth relation, for each version: 30.81% and 32.72%
The third relation has an extremely high uncertainty, at over 90%. Further, the distance values for each star themselves, do not vary much, and do overlap when the uncertainties are also considers. Some are more similar to each other, but this is also because of the uncertainty from the period.
Beginning with the biggest explanation for the large uncertainties: The most obviously inaccurate distance was the one calculated from equation 4.3; for every star, that relation gave the most different value and the biggest uncertainty, with every star having an uncertainty of about 96% and the distance itself was significantly different compared to the other relations for every star. So the question is, just what makes this relation so different from the others - with just looking at the equations, there is a simple explanation: it has the largest uncertainty in the slope and, in particular, the zero point.
The relation from Knapp et al. (2003) differs from the others because it is based off only Galactic Miras. Feast et al. (1989) derived it only from the LMC, Groenewegen and Whitelock (1996) used stars from the LMC to then apply the relation to the Galaxy and shifting the zero point without correcting for metallicity, and Whitelock et al. (2008) uses a similar process (from Groenewegen and Whitelock (1996)) but the zero point is found by using the *Hipparcos* parallaxes.
These different methods explain why the slope and the zero point in Knapp et al. (2003) in the most different with the highest uncertainty, and the large differences in these explain why the distances are not similar to the other relations as well as the large uncertainty.
From the other relations, the most recent one by Whitelock et al. (2008) would yield distances with the least uncertainty, although 30% is still significant and this quantity should be taken into consideration for all measurements in the galaxy and outside it that are based on the relation.

7. Acknowledgments

References

[1] Australia National Telescope Facility. *Pulsating Variable Stars*. URL: http://www.atnf.csiro.au/outreach//education/senior/astrophysics/variable_pulsating.html.

[2] Australia National Telescope Facility. *Variable Stars*. URL: http://www.atnf.csiro.au/outreach//education/senior/astrophysics/variable_types.html.

[3] M. W. Feast et al. "A period-luminocity-color relation for Mira Variables". In: *Mon. Not. R. astr. Soc.* 241 (1989), pp. 375–392.

[4] Michael Feast. *Mira Variables*. Encyclpedia of Astronomy and Astrophysics. Nature Publishing Group, 2001.

[5] M. A. T. Groenewegen and P. A. Whitelock. "A revised period-luminocity relation for Carbon Mira". In: *Mon. Not. R. astr. Soc.* 281 (1996), pp. 1347–1351.

[6] H. Karttunen et al. "Fundamental Astronomy". In: Springer-Verlag Berlin Heidelberg, 2007. Chap. 13.2.

[7] Sofie Liljegren. Licentiate Thesis.

[8] Sofia Ramstedt. PhD Thesis.

[9] G. R.Knapp et al. “Reprocessing the Hipparcos data of evolved stars III. Revised Hipparcos period-luminocity relationship for galactic long-period variable stars”. In: *A & A*. 403 (2003), pp. 993–1002.

[10] P. A. Whitelock. “The Period Luminocity Relation in Mira variables”. In: *AGB Stars and Related Phenomena*. Ed. by Toshiya Ueta, Noriyuki Matsunaga, and Yoshifusa Ita. National Astronomical Observatory of Japan. Mitaka, Tokyo, Japan: ASRP SOC/LOC, Nov. 2008.

[11] P. A. Whitelock, M. W. Feast, and F. van Leeuwen. “AGB variables and the Mira period-luminocity relation”. In: *Mon. Not. R. astr. Soc.*. 386 (2008), pp. 313–323.

8. Appendix

8.1. Other light curves plotted

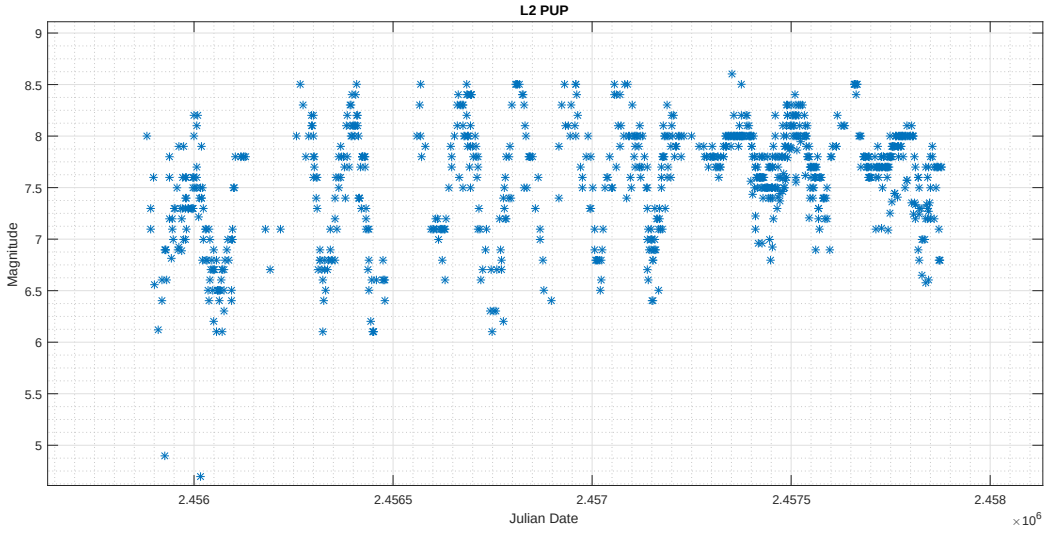

Figure 3: *L2 Pup light curve*

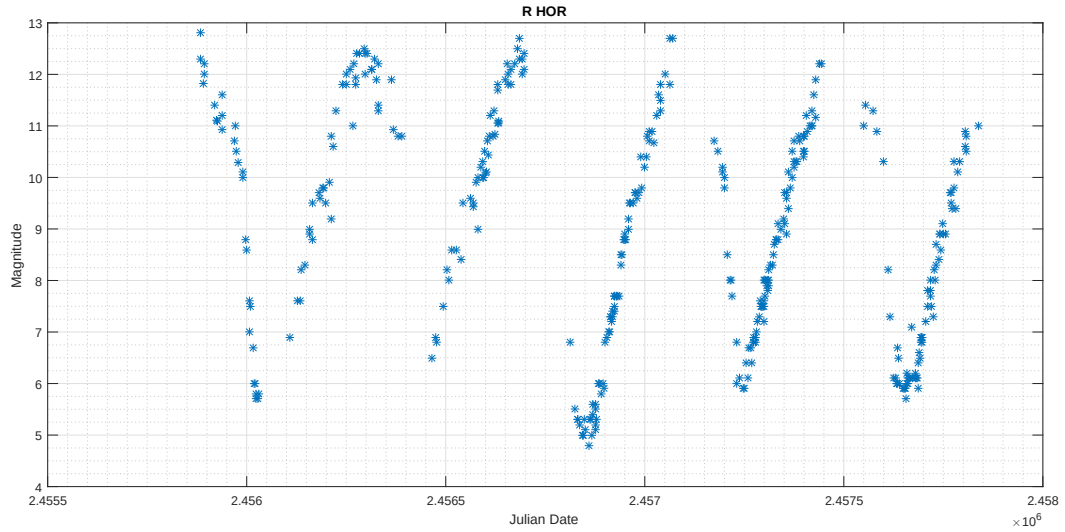

Figure 4: *R Hor light curve*

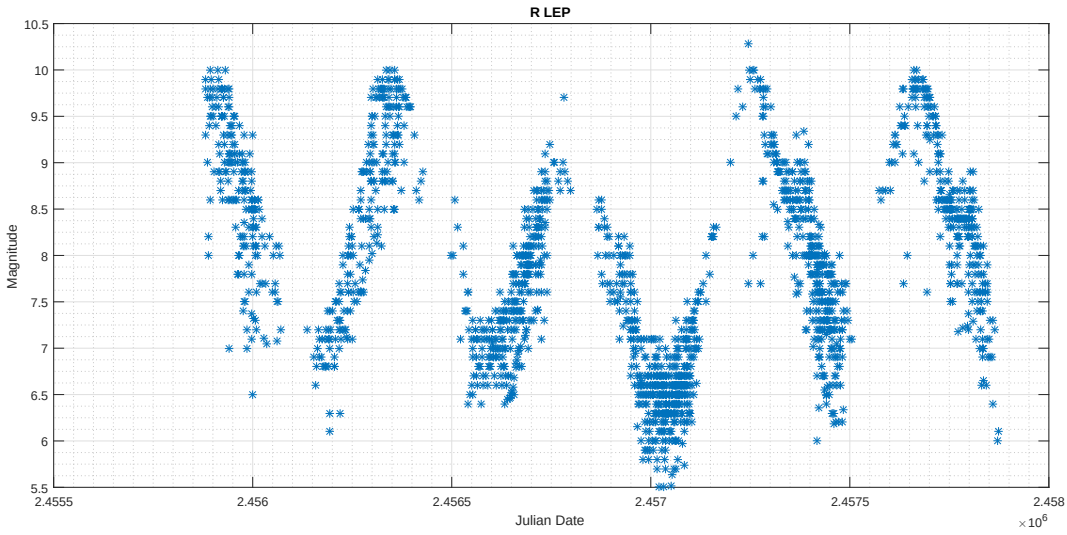

Figure 5: *R Lep light curve*

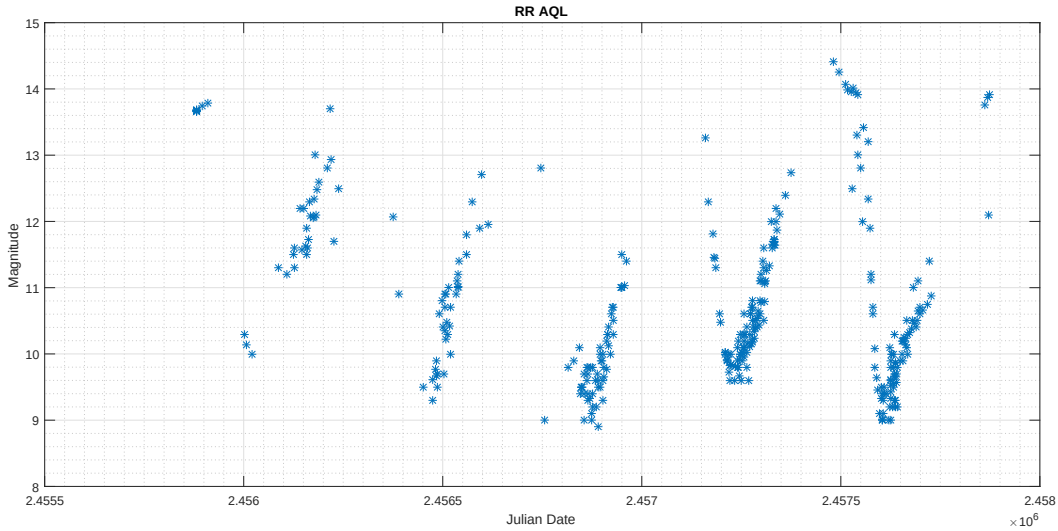

Figure 6: *RR Aql light curve*

Figure 7: *SW Vir light curve*

8.2. Uncertainties for remaining plots

Peak	Julian Date s
1	2457802 ± 12
2	2457660 ± 5
3	2457508± 9
4	2457356 ± 3
5	2457199± 12
6	2457081 ± 13

Table 19: *L2 Pup peak uncertainty*

Peak	Julian Date
1	2457838± 15
2	2457438± 6
3	2457063± 6
4	2456681± 5
5	2456295± 7
6	2455883 ± 1

Table 20: *R Hor peak uncertainty*

Peak	Julian Date
1	2457659 ± 9
2	2457245 ± 5
3	2456782± 10
4	2456345 ± 10
5	2455912 ± 12

Table 21: *R Lep peak uncertainty*

Peak	Julian Date
1	2457874± 13
2	2457482 ± 30
3	2457159± 40
4	2456746 ± 97
5	2456216 ± 75
6	2455909± 27

Table 22: *RR Aql peak uncertainty*

Peak	Julian Date
1	2457603 ± 24
2	2457387 ± 8
3	2457043± 9
4	2456810 ± 8
5	2456420 ± 35
6	2456028± 10

Table 23: *SW Vir peak uncertainty*

8.3. Light curved without measured period

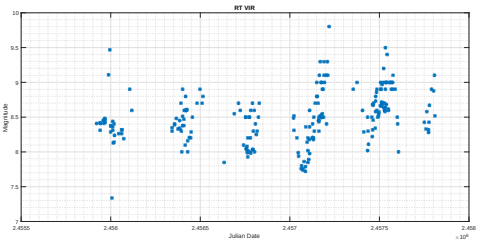

Figure 8: *RT Vir light curve*

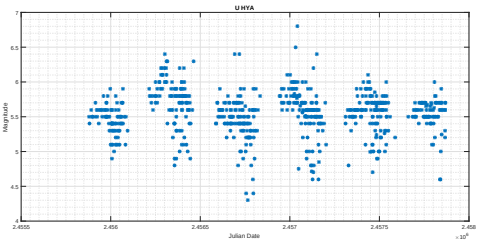

Figure 9: *U Hya light curve*

List of Figures

List of Tables